GROUTED MICROPILES FOR FOUNDATION REMEDIATION IN EXPANSIVE SOIL

John D. Nelson, Ph.D., D.GE.[1], Kuo-Chieh Chao, Ph.D.[2], Zachary P. Fox[3], and Jesse S. Dunham-Friel[4]

Abstract Foundation underpinning is a common component of remediation schemes for distressed foundations on expansive soils. For many applications in expansive soil, micropiles have distinct advantages over other techniques. This paper will concentrate on the design and construction of micropiles in expansive soil. It discusses the nature of building distress and the relationship between foundation movement and soil heave. It presents methods for determining the factors that are required for the design of micropiles. Such factors include calculation of expected free-field heave, depth of soil wetting, and prediction of pier movement. A finite element program developed by the authors and others to determine pier heave and internal forces is presented. The input parameters that are required for pier analysis are discussed, and the nature of the output and the sensitivity of the results to the output are described. Two case histories illustrate the application of the design method and the importance of construction methods on successful remediation and the advantages of micropiles over other methods. These case histories discuss the use of friction reducing casings and the importance of providing adequate connection of the micropiles to the foundation.

1. Introduction

Structural distress is commonly due to differential movement of building foundations due to heave of expansive soils. For foundations constructed on soils consisting of highly expansive clay, underpinning of the foundation is the most reliable method of remediation. Various underpinning methods that have been used include drilled piers, helical piles, push pins, and micropiles. Recently, micropiles have found increasing use, particularly in the Front Range of Colorado because of the reliability of the method and its ease of installation. The small size and versatility of the drilling equipment make micropiles well-suited for installation in places where access and mobility are limited. The drilling equipment is easily attached to existing foundations utilizing the weight of the structure for reaction. This makes the use of micropiles advantageous in places such as crawlspaces, garages, basements, and other confined areas.

[1] CEO and Principal Geotechnical Engineer, Engineering Analytics, Inc., and Professor Emeritus, Colorado State University, 1600 Specht Point Road, Suite 209, Fort Collins, Colorado, USA 80525. E-Mail: jnelson@enganalytics.com
[2] Vice President and Senior Geotechnical Engineer, Engineering Analytics, Inc., 1600 Specht Point Road, Suite 209, Fort Collins, Colorado, USA 80525. E-Mail: gchao@enganalytics.com
[3] Geotechnical Engineer, Engineering Analytics, Inc., 1600 Specht Point Road, Suite 209, Fort Collins, Colorado, USA 80525. E-Mail: zfox@enganalytics.com
[4] Geotechnical Engineer, Engineering Analytics, Inc., 1600 Specht Point Road, Suite 209, Fort Collins, Colorado, USA 80525. E-Mail: jdunham-friel@enganalytics.com

A typical micropile is constructed by first drilling a small diameter boring, generally 4 to 6 inches in diameter. A steel reinforcing bar is inserted and grout is tremied into the hole. A low

friction casing such as PVC may be inserted into the hole for the upper 10 to 50 feet to reduce uplift skin friction from the expansive soil. The capacity of the micropiles to support a structure and resist uplift forces is mobilized primarily through skin friction in the lower portions of the micropile.

Appropriate design of the micropiles involves careful site investigation, calculation of anticipated free-field heave, and then analysis of the required micropile length. The successful performance of the micropiles also involves careful attention to detail during construction.

The following sections present examples of the nature of distress caused by heave of expansive soil and typical foundation types that have been underpinned. They outline the geotechnical engineering parameters that are necessary for appropriate design and present methods for analysis of the micropiles. The input parameters required and methods of determination of these parameters are discussed. Important aspects of the construction are also discussed.

Two case histories are used to demonstrate important aspects of the remediation process. They demonstrate the advantages of micropiles in terms of ease of installation and reliability, and also serve to point out important aspects of construction.

2. Foundation Types and Nature of Distress

When expansive soils are encountered on a given site, foundation types that are commonly considered include drilled pier and grade beam systems or stiffened slabs-on-grade. Drilled pier and grade beam foundations isolate the structure from the expansive soils by creating a void space beneath the superstructure such that only the shaft of the drilled pier is in contact with the problematic soil. As will be discussed in greater detail later, uplift forces acting on the upper portion of a pier due to soil heave in the active zone are resisted by the embedment or anchorage zone below. There are many different types of reinforced or stiffened slabs-on-grade. In the United States, slabs are commonly stiffened by means of post-tensioning. Design methods vary in different areas of the world. The intent of the reinforced slab-on-grade is a slab foundation that is sufficiently rigid and stiff to minimize structural distortions to acceptable levels. Post-tensioned slabs-on-grade are typically designed for two conditions associated with expansive soils: (1) edge lift associated with seasonal moisture fluctuations, and (2) center lift associated with wetting beneath the center of the slab, or desiccation of soils around the perimeter of the slab during dry periods (Day, 1999). Distress in pier and grade beam foundations caused by expansive soils is typically the result of differential pier heave and manifests itself through cracking of the pier and/or grade beam causing distortion of the superstructure above. Figure 1 shows a grade beam that experienced diagonal cracking due to pier heave. Figure 2 shows a diagonal crack in a 30 inch diameter drilled pier near the intersection with the grade beam. In this case lateral forces were also imposed on the pier due to soil heave.

Figure 1. Grade beam crack due to void closure

Figure 2. Diagonal crack in a 30 inch drilled pier

Differential heave of the subsoil beneath slab-on-grade basement floors causes distortion of the slab which typically results in damage and distress to the structure above. Figure 3 shows a scenario where significant slab heave has necessitated the cutting of the interior wall studs in the basement of a residence to avoid lifting the first floor. Figure 4 shows a "center lift" condition in a basement slab-on-grade. The slabs-on-grade shown in Figures 3 and 4 were floor slabs and were not structural except to support the partition walls. The use of a stiffened slab as a foundation intends to minimize the differential movement shown in Figures 3 and 4.

Figure 3. Wall studs modified due to slab heave

Figure 4. Differential heave of basement slab

Regardless of the foundation type, distress associated with expansive soils typically results in significantly increased maintenance and repair costs throughout the life cycle of the structure. Additionally, differential movements result in racked doors and windows which in addition to inconvenience, may result in loss of emergency egress. As a result of such distress and losses of functionality, foundations are often underpinned with structural elements such as micropiles.

3. Design of Micropiles in Expansive Soils

Micropiles have been used to underpin foundations since the early 1950s and they are increasingly being used for underpinning foundations experiencing heave due to expansive soils. Despite their increasing usage, there is a lack of published literature regarding micropile design, installation, or performance in expansive soils. The following offers a method for analysis of the behavior of micropiles installed in expansive soils.

Heave Prediction

Free-field heave distribution with depth is the primary data on which pier heave is calculated. Therefore, a review of free-field heave calculations is presented below.

Various heave prediction methods have been developed based on results of one-dimensional oedometer tests (Fredlund et al. 1980; U.S. Army Corps of Engineers, 1983; Nelson and Miller, 1992; Fredlund and Rahardjo, 1993; Fredlund et al. 2012). These methods utilize the net mechanical stress, $\sigma' = (\sigma - u_a)$, and the matric suction; $h = (U_a - U_w)$ as the stress state variables. In these variables, σ is the total stress and U_a and U_w are the pore air and pore water pressures. The soil heave takes place as the suction is decreased. These methods are commonly referred to as "oedometer" methods. The oedometer methods all use the same basic equation for calculation of heave. The equation for heave of a soil layer of thickness, Δz_i, subjected to an applied stress, $\Delta\sigma'_v$, is

$$\rho_i = C_H \cdot \Delta z_i \log\left[\frac{\sigma'_{vo} + \Delta\sigma'_v}{\sigma'_{cv}}\right]_i \quad (1)$$

and the heave of the entire soil column is,

$$\rho = \sum_{i=1}^{n} \rho_i \quad (2)$$

where: ρ = free-field heave; Δz_i = thickness of each soil layer; σ'_{vo} = overburden stress; $\Delta\sigma'_v$ = applied stress; σ'_{cv} = constant-volume swelling pressure, and C_H = constitutive parameter.

The parameter C_H defines the amount by which a soil sample will swell when it becomes wetted. The method presented here is characterized by the manner in which the C_H parameter is determined. It considers both the change in suction due to wetting and the applied stress that is acting on the soil when it is wetted.

The determination of C_H is depicted in Figure 5 which is a three dimensional plot of the stress paths followed during the inundation and heave of a soil. In a conventional consolidation-swell oedometer test, a sample of soil is consolidated under an inundation stress, labelled as σ'_i in Figure 5. The initial state of the soil under the inundation stress, σ'_i, is represented by the point labeled K. At that point the soil suction is equal to some value labelled as h_{c1}. The initial percent swell, $\varepsilon_{s\%}$, at point K (and H) is equal to zero. When the sample is inundated, the suction is reduced to h_o and the soil swells along the path KB. The projection of that stress path on the

plane defined by the axes for $\varepsilon_{s\%}$ and log σ' is the line GB. The sample is then loaded back to its original height along the path BA. The value of stress corresponding to point A is the consolidation-swell swelling pressure, σ'_{cs}.

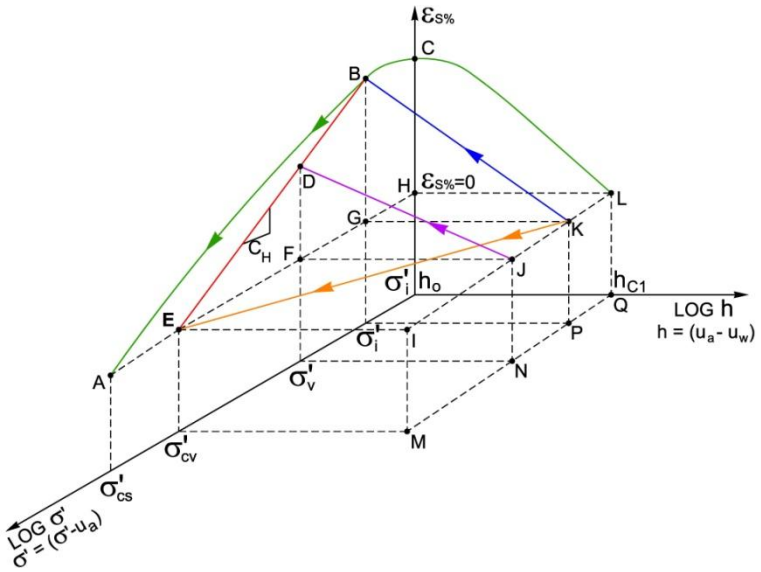

Figure 5. Stress Paths for Soil Expansion

In a conventional constant-volume oedometer test, the sample begins at point K but because it is constrained from swelling it develops a confining stress as the suction decreases to h_o and the stress path would be along a line such as KE. The value of stress corresponding to point E is the constant-volume swelling pressure, σ'_{cv}. Due to hysteretic effects, the value of σ'_{cv} is generally less than that of σ'_{cs}. The reason for this is somewhat intuitive in that it should be easier to prevent water molecules from entering into the soil lattice than to force the water out once it has entered into the soil. A full understanding of all of the factors contributing to the hysteresis is not known. However, one reason for this hysteresis is believed to be the result of the fact that soil expansion takes place in two distinct ways. Initially the expansion is due to hydration of adsorbed cations on the soil particles. This is "crystalline" expansion. After which the expansion is a result of "osmotic" expansion in which the soil is probably developing a diffuse double layer (Norrish, 1954).

For general purposes, one could argue that a sample inundated at σ'_{cv} would exhibit no swell. This assumption is accurate enough for purposes of computing heave, although non-linearity and secondary effects may indicate that this is not exactly true. For an element of soil in the ground, the initial stress conditions could be at some point such as J. When that sample is inundated it will swell along a stress path such as JD. Point D will fall between points B and E. Our experience and data has shown that the line BDE is close to being a straight line (Justo et al. 1984; Reichler, 1997; Nelson et al. 2006; Fredlund et al. 2012). Thus, the slope of the line BDE

defines the constitutive relationship between the percent swell, $\varepsilon_{s\%}$, that a soil will undergo, and the stress at which it is wetted. The slope of that line is C_H.

It is important to note that, as shown in Figure 5, the line BDE which defines C_H represents the expansion, or heave, that will occur due to suction changes under different values of applied stress. Thus, it is a constitutive relationship that incorporates both of the independent stress state variables, σ' and $(u_a - u_w)$, for use in computing heave.

For practical purposes, it is not necessary to plot the entire three dimensional stress paths in order to determine C_H. Figure 6 shows the projection of the stress paths shown in Figure 5 onto the $\varepsilon_{s\%}$ and log σ' plane. The results of both consolidation-swell test and constant-volume test are shown as the lines GBA and GFE, respectively.

The heave index, C_H, is the slope of the line BDE in Figure 6 and is equal to:

$$C_H = \frac{\varepsilon_{s\%}}{100 \times \log\left(\frac{\sigma'_{cv}}{\sigma'_i}\right)} \qquad (3)$$

where $\varepsilon_{s\%}$ is the percent swell corresponding to σ'_i expressed as a percent, and σ'_i is the vertical stress at which the sample is inundated.

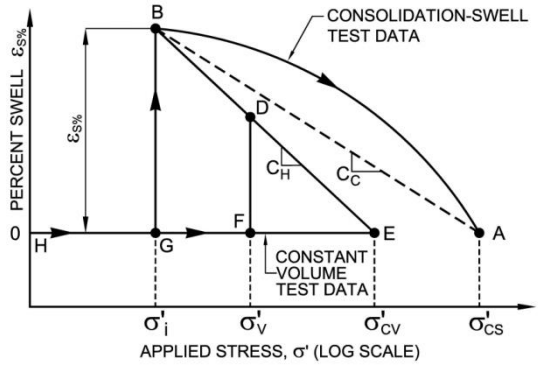

Figure 6. Determination of Heave Index, C_H

The method for prediction of free-field heave presented above is essentially the same as Method A in the ASTM Standard D4546-08 as is discussed in Nelson et al. (2012a).

The value of C_H can be determined from the results of a consolidation-swell test and a constant-volume test using identical samples of the same soil. However, in practice it is virtually impossible to obtain two identical samples from the field. Therefore, it is convenient to utilize a relationship between σ'_{cs} and σ'_{cv} such that C_H can be determined from a single consolidation-swell test. On the basis of data that has been assembled from a number of different sources, it

was found that experimental data corresponded well to Equations 4a and 4b. The authors have found that for use in the Front Range area of Colorado a value of λ_{log} of 0.6 is reasonable when Equation 4a is used or a value of $\lambda_{arithmetic}$ of 0.3 is reasonable when Equation 4b is used. However, for application of these equations to a particular soil type, it would be prudent to perform tests to determine an appropriate value for that soil (Nelson et al. 2012a).

$$\log \sigma'_{cv} = \log \sigma'_{i} + \lambda_{log} (\log \frac{\sigma'_{cs}}{\sigma'_{i}}) \quad (4a)$$

$$\sigma'_{cv} = \sigma'_{i} + \lambda_{arithmetic} (\sigma'_{cs} - \sigma'_{i}) \quad (4b)$$

Soil Contributing to Heave Zone

The depth of soil that is contributing to heave at a particular point in time depends on two factors. These are the depth to which water contents in the soil have increased since the time of construction, and the expansion potential of the various soil strata. As water migrates through a soil profile different strata become wetted, some of which may have more swell potential than others. Consequently, the zone of soil that is contributing to heave varies with time.

The amount of heave that will occur at a particular time depends on the manner in which the groundwater migrates in the soil and the expansion potential of the soil at depth. Movement of the soil surface will begin almost immediately after construction, whereas some time will be required for the soil at deeper depths to become wetted. Thus, the surface of the soil will begin to heave almost immediately, but movement of piers will be delayed, sometimes by several years.

The term "active zone" has been in common usage in the field of expansive soils. However, the usage of that term has taken different meanings at different times and in different places. Therefore, for purposes of clarity and consistency, the following five definitions have been put forth (Nelson et al. 2001).

Active Zone, Z_A, is that zone of soil that is contributing to heave due to soil expansion at a particular point in time.

Zone of Seasonal Moisture Fluctuation, Z_s, is that zone of soil in which water contents change seasonally due to climate changes.

Zone of Wetting, Z_w, is that zone in which water contents have increased beyond the pre-construction conditions.

Depth of Potential Heave, Z_p, is the depth to which the overburden vertical stress equals or exceeds the swelling pressure of the soil. This represents the maximum depth of Active Zone that could occur.

Design Active Zone, Z_{DA}, is the zone of soil that is expected to become wetted during the design life of the structure. It may be less than the depth of potential heave if water migration analyses indicate that the entire depth of potential heave will not become wetted. If water migration analyses are not available and if the depth of potential heave is of reasonable value for design, it is prudent to assume the depth of the design active zone is equal to the depth of potential heave.

Construction of buildings and pavements in arid regions typically results in a reduction of evapotranspiration from the soil. Additionally, the introduction of irrigation typically exceeds the evapotranspiration of the vegetation. These factors as well as others result in the development of a wetting front that progresses downward in the soil. Below the wetting front, the water content is the same as that which existed prior to introduction of the water source. However, above the wetting front, the water contents are higher and the soil may be saturated or unsaturated. The difference in soil suction between the wetter and drier zones will result in downward flow of water, and the wetting front will continue to move downward until an impermeable boundary or a water table is reached (McWhorter and Nelson, 1979). Once an impermeable boundary is reached, the water table will propagate upward to the surface, thusly, forming a perched water table. Full wetting of the soil profile would be expected to occur if the soil above the wetting front is saturated and the wetting front advances to below the depth of potential heave. Where a rising groundwater table is anticipated, the full wetting conditions should be used to make calculations (Houston et al., 2001).

If full wetting is not expected to occur, analyses must be conducted to determine the water content profile at the end of the design life. If such analyses are not conducted it should be assumed that full wetting will occur to the depth of the design active zone.

For sites at which the depth of potential heave is large, the degree of wetting typically will be less than fully saturated (Chao et al. 2006; Overton et al. 2006). Design of foundations for these conditions must consider the design life of the structure, the depth of wetting that can occur during the design life, the degree of saturation and thus the portion of potential heave that can develop during the design life.
The depth of wetting and corresponding degree of saturation can be calculated using readily available software, such as VADOSE/W, SVFlux, or Hydrus 2-D. Using the results of these analyses, the amount of heave that is expected to occur in the partially wetted zone can be calculated. This amount of heave will be less than that calculated assuming full wetting for the entire depth of potential heave.

Pier Heave Calculations

The earliest method used to design piers in expansive soil is termed the "Rigid Pier" method. This method assumes that the pier will not move and determines a required pier length by equating the negative, or downward, skin friction below the depth of the design active zone, plus the dead load, to the uplift pressures exerted on the pier by the swelling soil. Chen (1965), O'Neill (1988), and Nelson and Miller (1992) present methods for rigid pier analysis in

expansive soil. Rigid pier design generally produces conservative pier lengths for a light structure founded on a deep deposit of highly expansive soil. The rigid pier design works well if the stratum of expansive soil is not thick and is underlain by a stable non-expansive stratum. However, in a deep deposit of expansive soil, the required pier length approaches a value equal to twice the depth of the design active zone. In such cases the design rigid pier length is generally not practical for a light structure.

In reality almost all structures are able to tolerate some amount of pier heave. The amount of tolerable heave to be used for design depends on the nature of the structure. Methods of analysis of pier heave were developed by Poulos and Davis (1980) and were adapted by Nelson and Miller (1992) to develop design charts for calculating pier heave. This method is termed the "Elastic Pier Method". The elastic pier method calculates the pier heave assuming the pier is a stiff inclusion in an elastic half space. Nelson et al. (2007) further refined this method and presented design charts for straight-shaft and belled piers. The elastic pier method was developed for piers with uniform properties with depth installed in a uniform soil profile. Additionally, the elastic pier analysis formulation breaks down when the length to diameter ratio becomes too great. Micropiles typically have non-uniform properties with depth, are often installed in non-uniform soil profiles, and have large length to diameter ratios. Therefore, the elastic pier method is not well suited for their analysis.

Finite element approaches to pier analyses provide versatility to consider such details as non-uniform soil or pier interface properties with depth and large length to diameter ratios. Finite element numerical analysis of pier heave in expansive soils has been proposed previously by several authors in the literature (Amir and Sokolov, 1976; Lytton 1977; Justo et al. 1984; Abdel-Halim and Al-Qasem, 1995; Mohamedzein et al. 1999). However, the methods presented in the literature do not discuss in detail how the finite element based solution was formulated or used. Nelson et al. (2012b) presents one such finite element based numerical analysis approach termed APEX for Analysis of Piers in EXpansive Soils. The formulation of this finite element based approach is discussed below.

APEX Formulation

The APEX formulation is discussed in detail in Nelson et al. (2012b) and is briefly summarized below. Swell is assumed to be isotropic and it is simulated using conventional analyses of thermal strains in solids. The constitutive equations are as follows:

$$\varepsilon_{rr} = \frac{1}{E}\left[\sigma_{rr} - \nu\ \sigma_{\theta\theta} + \sigma_{zz}\ \right] + \varepsilon_{iso} \qquad (5)$$

$$\varepsilon_{\theta\theta} = \frac{1}{E}\left[\sigma_{\theta\theta} - \nu\ \sigma_{zz} + \sigma_{rr}\ \right] + \varepsilon_{iso} \qquad (6)$$

$$\varepsilon_{zz} = \frac{1}{E}\left[\sigma_{zz} - \nu\ \sigma_{rr} + \sigma_{\theta\theta}\ \right] + \varepsilon_{iso} \qquad (7)$$

where: ε_{iso} = isotropic swelling strain; and ε_{rr}, $\varepsilon_{\theta\theta}$, ε_{zz} = components of stress and strain in cylindrical coordinates. The pier-soil interface is accounted for with a mixed boundary condition. The mixed boundary condition is shown in Figure 7 and can be written as follows:

$$F_t = k\ H_p - U_t \qquad (8)$$

where: F_t = nodal force tangent to pier; H_p = pier heave; U_t = nodal displacement tangent to pier; and k = parameter used to adjust shear stress, which serve a purpose similar to a spring constant.

Figure 8 depicts the manner in which APEX calculateds pier heave. The pier is modeled as a rigid body connected to an elastic, expansive medium by springs with a spring constant k. Figure 8a illustrates the conditions before swell takes place when there are no uplift forces on the pier. Figure 8b illustrates the conditions after swelling takes place but before any pier heave, when the shear forces exerted on the pier result in an upward force on the pier. At this point the pier is not in equilibrium, and the pier is then allowed to move up until forces are balanced. Figure 8c illustrates the condition after forces are balanced and the pier is in equalibrium. The forces are balanced during each iteration by adjustment of the "spring constant" k.

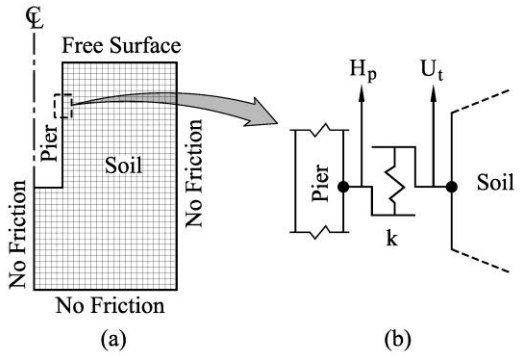

Figure 7. Boundary Conditions: (a) Soil Boundary, (b) Mixed Boundary (after Nelson et al. 2012b)

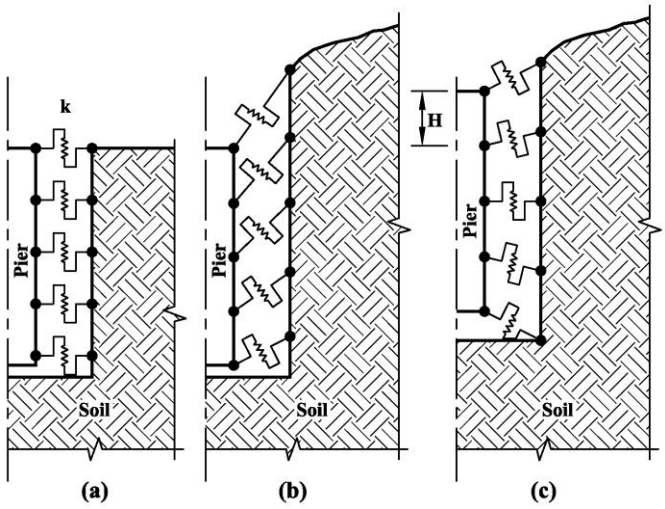

Figure 8. Schematic of pier and soil interface: (a) initial-no force on pier, (b) soil heave-upward force on pier, (c) pier heave-resultant force on pier is zero (after Nelson et al. 2012b)

The APEX formulation allows for movement between the pier and the expansive soil mass by either slip between the pier-to-soil interface or failure of the soil adjacent to the pier. Prediction of the controlling failure mechanism is difficult as it depends on the normal stress. Therefore, the slip and soil failure mechanisms are calculated at each iteration. Figure 9 illustrates the allowable shear stress as a function of the normal stress for both mechanisms.

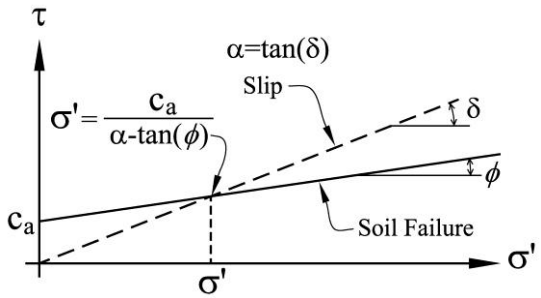

Figure 9. Strength Envelopes for Slip and Soil Failure Modes (after Nelson et al. 2012b)

Input Parameters for APEX

The soil and heave profiles are the primary input parameters used in the APEX analysis. Detailed and accurate characterization of the soil profile to the full depth to which the soil will influence the behavior of the piers is a critical element of pier design. If the depth of exploration is too shallow, or if an insufficient number of samples are collected and tested, variations in the soil profile will not be detected. Figure 10 shows four examples of soil profiles that are typical of those encountered at expansive soil sites in the Front Range Area of Colorado.

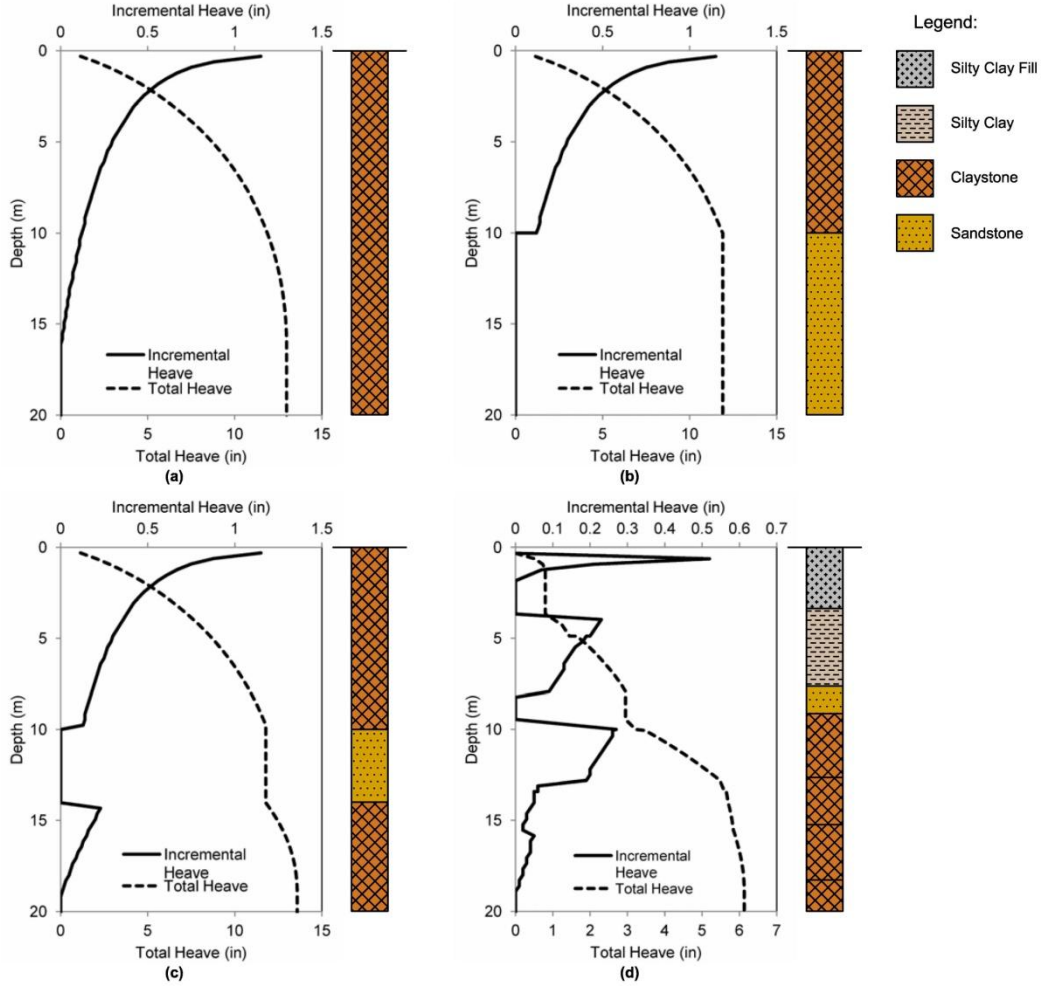

Figure 10. Examples of soil and heave profiles: (a) uniform expansive soil, (b) expansive soil over non expansive soil, (c) expansive soils with sandstone layer between, (d) complex soil profile

Figure 10a illustrates a simplified soil profile where one relatively uniform expansive soil such as clay or claystone is encountered to the full depth of exploration. In this case the incremental heave is high at the surface and decreases exponentially with depth to the depth of potential heave. Figure 10b illustrates another simplified soil profile where an expansive soil is underlain by a non-expansive soil such as sandstone. Relatively uniform soil profiles such as those shown in Figure 10a and 10b are rarely encountered in the field. Instead it is typical to encounter multiple soil layers with varying expansion potential such as in the profiles shown in Figures 10c and 10d. Figure 10c illustrates a soil profile that consists of three primary soil layers where an expansive soil layer is underlain by a non-expansive soil which is underlain by more expansive soil. Figure 10d illustrates a complex soil profile which is typical of many expansive soil sites in the Front Range Area of Colorado. The soil profile shown in Figure 10d has multiple layers with varying expansion potential. Accurate analysis of pier heave constructed in complex soil profiles such as these require a detailed analysis which can account for the variations in heave with depth. Incremental free-field heave computed for such profiles is the most important input parameter in the APEX analysis. The free-field heave profile can be determined by predicting heave versus depth as discussed in the above sections, taking into account overburden stresses and anticipated wetting profile.

The primary elastic input properties used in APEX analysis are the Young's modulus (E), Poisson's ratio (ν), and coefficient of lateral stress (K_o). An example pier was analyzed by Nelson et al. (2012b) to demonstrate the effect that changes in the values of E, ν, and K_o have on heave and tensile force in the pier. The results of these analyses are shown on Figure 11.

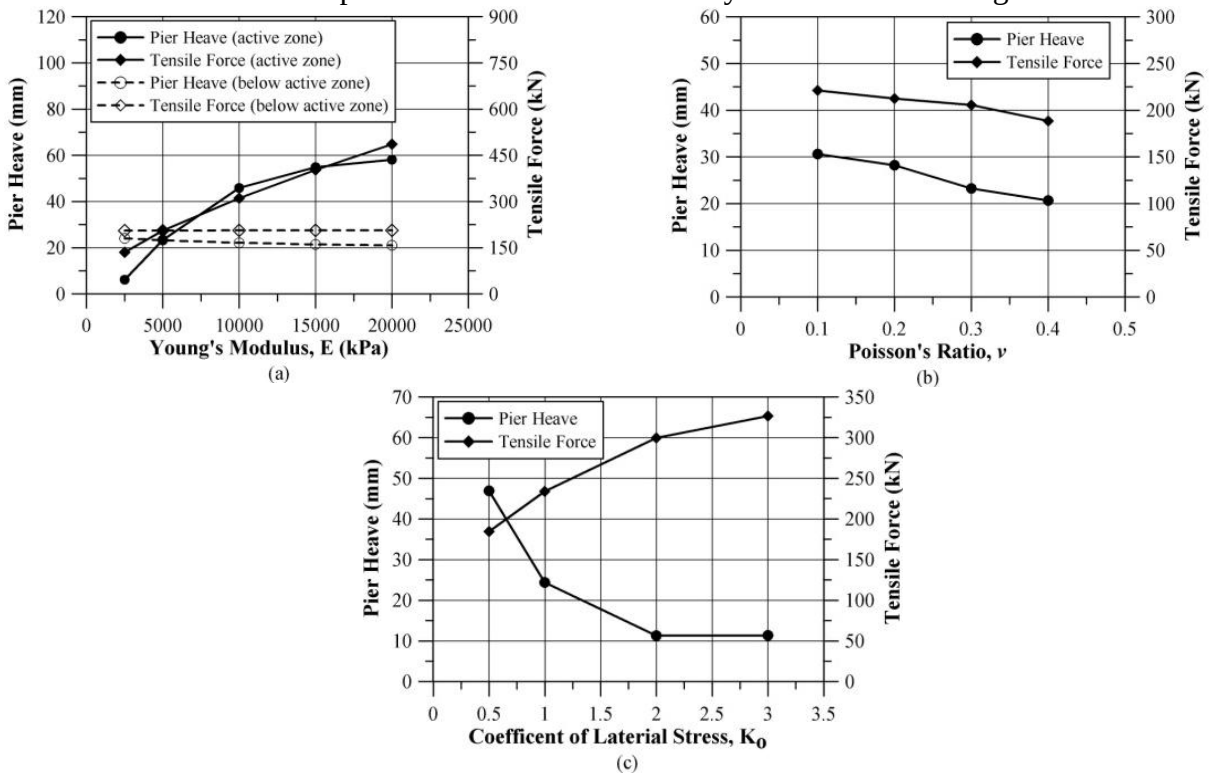

Figure 11. Effect of Soil Elastic Properties on Heave and Tensile Force (a) Young's Modulus (b) Poisson's Ratio (c) Coefficient of Lateral Stress (after Nelson et al. 2012b)

Figure 11a shows that an increase in E of the active zone results in a significant increase in both the pier heave and in the tensile forces developed in the pier. However, changes in E below the active zone produce negligible effect on the heave or tensile force. Figure 11b shows that an increase in the value of Poisson's ratio has some impact on the pier heave and the tensile force but the impact is not nearly as great as that of the value of E in the active zone. Figure 11c shows that an increase in the coefficient of lateral stress, K_o, results in a decrease in pier heave and an increase in pier force. The analysis is sensitive to the value of K_o.

The value of E varies significantly with soil water content. Thus, E should be determined for the entire range of water contents that are expected to occur during the design life of the micropiles. The value of E at the water content during site investigation and prior to wetting can be calculated from unconfined compression, triaxial or oedometer tests performed at the in-situ water content. The value of E at saturated conditions can be determined using results of triaxial or oedometer tests. It is convenient to use the results of the oedometer tests to measure the elastic modulus along with the expansive properties. The slope of the line BA in Figure 6 represents an average value of the coefficient of compression, C_c, and can be used to determine the confined modulus, M, and then relate that to E. A method for determination of E by determining the constrained modulus (M) and converting it to E is presented in Lambe and Whitman (1969).

The value of ν has a relatively minimal impact on the pier heave and tensile force and can therefore be estimated using typical values for the expansive medium. Alternatively, the value of ν can be measured by conducting unconfined compression or triaxial tests with radial strain measurements.

The value of K_o should be accurately determined. Nelson et al. (2012b) discusses correlations presented in Lambe and Whitman (1969) between the K_o and index properties of the soil that can be used to determine reasonable values for use in design.

Example calculations performed by Nelson et al. (2012b) have demonstrated that changes to α do not substantially affect the calculated pier heave but do have a significant impact on the tensile force in the pier when the frictional interface is uniform with depth. However, if the upper portion of the micropiles installed in expansive soils is sleeved with PVC, the frictional properties for each part require accurate determination of the value for α with depth along the micropile. The APEX analysis developed by the authors and others allows for α to be changed with depth in order to allow for accurate representation of the frictional properties at all locations along the micropile.

The frictional interfaces that typically occur during the construction of micropiles in expansive soils are soil to grout, grout to PVC, and PVC to soil as is discussed in Schaut et al. (2011). The values of α presented in the literature for a concrete to soil interface generally range from 0.1 to 0.25 (Chen, 1988; O'Neill, 1988; Sorochan, 1991; Nelson and Miller, 1992). However, field test results presented by Benvenga (2005) indicate that α generally ranges from about 0.4 to 0.6 and can be as high as 0.9. Schaut et al. (2011) completed testing on the soil to grout interface as well as the grout to PVC and PVC to soil interfaces using typical micropile construction materials and claystone soil from the Front Range Area of Colorado. The results of this research indicate that the value of α depends on the method of testing, whether the soil is remolded and what the water content of the soil is during testing. It was shown that PVC casing reduces the frictional

resistance along the cased section of the micropile. The data presented in Schaut et al. (2011) are presented in Table 1.

Table 1. Summary of Micropile Interface Strength Data (after Schaut et al. 2011)

Interface	Direct Shear Testing				Modified Triaxial Testing			
	δ_p	c_p (psf)	δ_r	c_r (psf)	δ_p	c_p (psf)	δ_r	c_r (psf)
Grout-to-PVC (Smooth, Dry)	16.3°	0	11.7°	0	12.8°	0	10.1°	0
Grout-to-PVC (Rough, Dry)					20.1°	0	15.3°	0
Soil (Remolded)-to-PVC (In-Situ Water Content)	16.6°	923	15.1°	700				
Soil (Remolded)-to-PVC (Inundated)	18.6°	0	15.4°	0				
Soil-to-PVC (In-Situ Water Content)					11.2°	0	9.7°	0
Soil-to-Grout (In-Situ Water Content)	20.0°	2,231	16.4°	1,296				
Soil-to-Grout (Inundated)	19.8°	1,314	14.5°	851				

Output Results from APEX

Typical APEX input and output for a soil profile is presented on Figure 12. Figure 12a shows the heave profile input into the APEX program. Figure 12b shows the distribution of slip along the pier. This figure indicates that for this case, slip was the failure mechanism along the entire length of the pier and therefore soil failure was not experienced. Figure 12c shows the distribution of shear stress along the pier with positive shear stresses in the anchorage zone and negative shear stresses in the uplift zone. Figure 12d shows the axial force in the pier with the maximum value occuring at the interface between the uplift and anchorage zones.

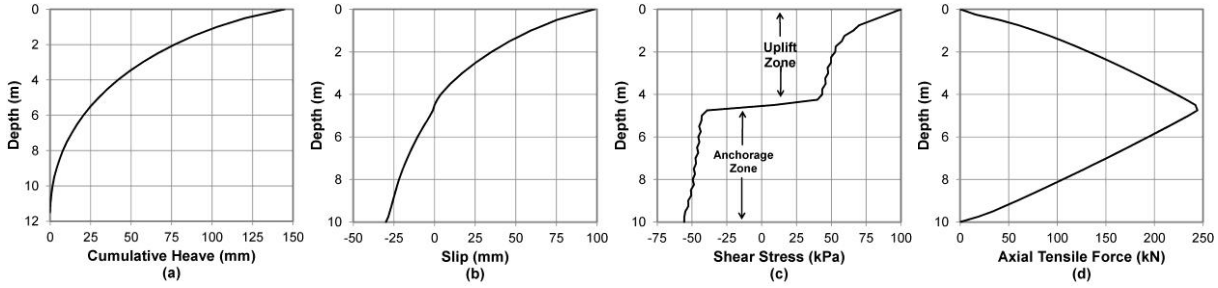

Figure 12. Typical output from APEX Program: (a) cumulative heave used as input, (b) variation of slip along pier, (c) shear stress distribution along pier, (d) axial force distribution (after Nelson et al. 2012a)

Pier Design Charts

An example of a pier design chart that was derived using the results of APEX analyses is shown in Figure 13. This design chart was developed using an α value equal to 0.4 held constant over the entire depth. Design charts of this nature can be developed using APEX and can be used to design micropiles.

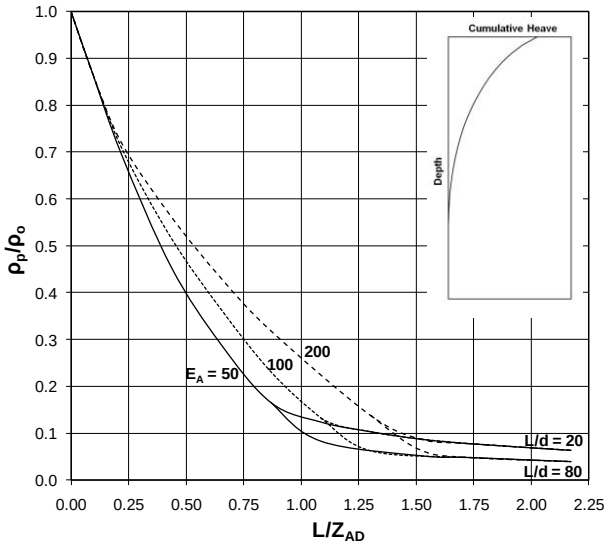

Figure 13. Pier heave versus pier length - nonlinear free-field heave (after Nelson et al. 2012a)

4. Micropile Types and Typical Construction in Expansive Soil

Micropiles have been classified into five different types based on construction technique (FHWA, 2005 and AASHTO, 2012). The five micropile types are shown in Figure 14.

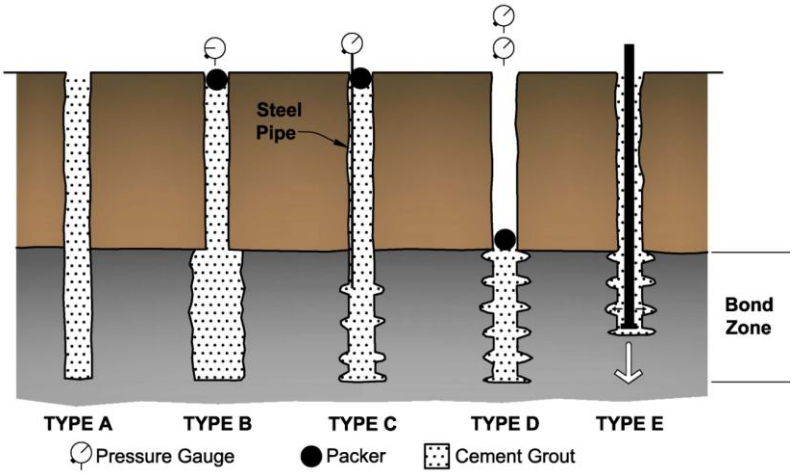

Figure 14. Five micropile construction techniques (after FHWA, 2005 and AASHTO, 2012)

A typical micropile installed in expansive soil has a configuration similar to Type A shown in Figure 14 with details shown in Figure 15. The upper portion of the micropile is cased with a PVC sleeve while the bottom portion has grout in direct contact with the soil. Depending on the method of construction and the fit between the PVC casing and the drilled hole, grout can flow

up in the annulus between the PVC and the side of the hole as shown on Figure 15. An all thread bar is typically used for to reinforce the micropile and provide a means for attachment to the foundation.

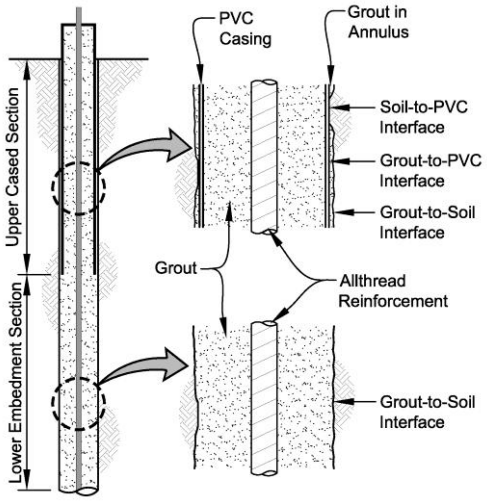

Figure 15. Schematic of typical micropile in expansive soil (after Schaut et al. 2011)

Figure 16. Micropile drill rig bolted to grade beam foundation

Micropiles used in expansive soils typically consist of drilling a 4 to 6 inch hole using a hydraulic drill rig that mounts to the foundation as shown in Figure 16. After drilling, casing made of rigid PVC pipe or other material is placed in the open hole in order to reduce the friction between the micropile and the surrounding expansive soil. Figure 17 shows PVC casing placed in the drilled hole prior to grout placement. Micropiles are typically tremie grouted from the bottom of the hole which often allows the grout to flow up the inside of the PVC casing as well as into the annulus between the side of the hole and casing as discussed in Schaut et al. (2011). Soil swelling or worn cutting teeth on the auger bit may restrict flow of grout into the annulus between the soil and the casing. Figure 18 shows a micropile during tremie grouting. After curing of the grout, the micropile is then connected to the bracket.

Figure 17. Micropile prior to grouting with annulus around the outside of casing

Figure 18. Micropile during grouting. Note that the grout is tremied into the hole

5. Case Histories

The following case histories from sites in the Front Range Area of Colorado illustrate the advantages of micropiles and also serve to point out important aspects of construction.

Private Residence in Loveland Colorado

An interesting case history regarding the use of grouted micropiles in the remediation of distressed structures is the case of a single family home originally constructed on spread footings in Loveland, Colorado during the summer of 1995. After the original homeowners reported evidence of structural distress, local geotechnical and structural engineering firms were hired to investigate potential causes. Results of their investigations indicated that differential movement of the expansive soils beneath the residence had resulted in the basement and garage slabs being 6.75-in and 7.0-in out of level, respectively. The respective reports recommended underpinning of the residence and a number of alternative underpinning methods were proposed including helical piers, push-pins, straight shaft piers and micropiles. A combination of steel push-pins and helical piers were ultimately used to underpin the residence during the winter of 2001. The push pins and helical piers were recommended to be installed to a minimum depth of 30 ft. In 2010, continuing structural distress was observed by the homeowners and measured by performing inverted joist level surveys of the basement and garage. Figures 19 and 20 illustrate some of the observed distress experiences to the residence in 2010 after initial underpinning.

Figure 19. Diagonal Brick Cracking

Figure 20. Diagonal Drywall Cracking

The lack of as-built information regarding the installation of the steel push-pins and the nature of the distress caused suspicion that the push-pins may not have been installed to the depths specified. To investigate, a geophysical survey was conducted by Zonge International, Inc. using a magnetic difference meter and a conductivity meter. In order to conduct the survey, a micropile drill rig was used to drill 4-in diameter holes to a depth of 35 ft adjacent to three existing push-pins and one helical pier. The boreholes were cased with PVC pipe and the geophysical meters were inserted into the boreholes allowing data collection at 1 ft intervals along the entire length of the boreholes. Figure 21 shows the magnetometer/conductivity probe with the PVC-cased borehole in the background. Results of the geophysical survey clearly showed that the depth of the push-pin piers and helical piers ranged from 9 to 21 ft, significantly less than the depth specified. Due to the very hard state of the claystone beneath the residence it was not possible to install the push-pins and helical piers to the depths specified. The micropile drill rig used in this investigation secured to the foundation in order to drill in the hard claystone. The fact that the exploratory holes for the geophysical testing were drilled to a depth of 35 ft

using micropile technology shows that grouted micropiles could have been drilled and installed to the depths specified in the underpinning plans. In contrast, push pins and helical piers were not been able to be successfully installed to the depths specified, thereby significantly reducing their ability to resist uplift caused by heave of the expansive soils. This case study demonstrates the advantage of micropiles as compared to other underpinning options for use in hard expansive soil conditions.

Figure 21. Magnetic Gradiometer, Testing Apparatus and Cased Hole

Vista Ridge Subdivision in Erie, Colorado

Grouted micropiles were used to underpin foundations in expansive soils in two adjacent subdivisions along the Front Range of Colorado. The two subdivisions contain 80 homes, most of which were recommended to be underpinned due to intolerable foundation movements and unacceptable predicted future heave calculated for the site. The residences were originally constructed on pier and grade beam foundations with straight shaft piers 25 ft deep. Approximately 30 micropiles were installed beneath each residence and the existing piers were cut off from the grade beam. Over two years after underpinning was complete and interior cosmetic repairs had been made, new and ongoing structural movements were observed in some, but not all of the residences which had been underpinned. Distress manifested as apparent "dishing" of the residences with the exterior perimeter appearing to be higher than the center of the residences. Upon inspection of the micropiles and micropiles brackets, gaps were observed between the micropiles and micropile brackets or between the micropile brackets and the foundation grade beams. This was only observed in micropiles along the exterior perimeter of the residences. Figure 22 shows a separation observed between the micropile and the micropile bracket as indicated by the gap in the shims. Figure 23 shows a separation observed between the grade beam and the micropile brackets.

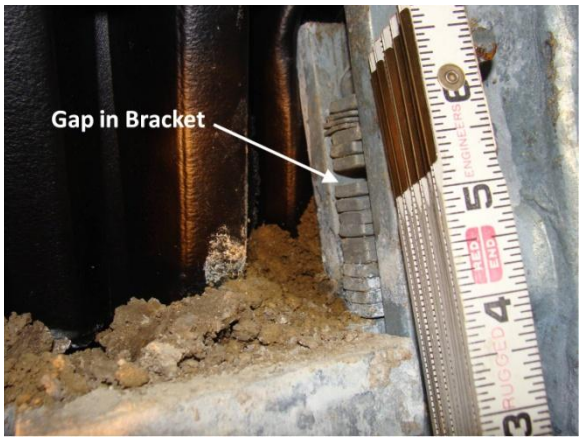

Figure 22. Separation in bracket shims

Figure 23. Grade beam lifting off bracket

Potential uplift forces acting on the foundation walls from upward movement of the adjacent backfill material resulting from heave of the expansive soil beneath the backfill zone were calculated and compared to the design dead loads for the micropiles. The uplift forces acting on the foundation wall due to friction between the backfill and the wall were essentially equal to or greater than the dead loads on the micropiles. In other words, the vertical movement of the foundation backfill along the vertical interface of the foundation wall had the capability of lifting the structure off of its foundation if no positive connection between the micropile and grade beam was established. Two different micropile bracket types had been used with the micropiles as shown in Figures 24 and 25. Only the micropile bracket shown in Figure 25 had been connected to the grade beam. For the bracket shown in Figure 24, the weight of the structure was the only force maintaining contact between the grade beam and the brackets. The most likely explanation for the observed distress was the lifting of the perimeter foundation walls due to heave of the expansive soils beneath the backfill zone along the exterior foundation walls.

Figure 24. Micropile Bracket A

Figure 25. Micropile Bracket B

To correct the situation, the micropile brackets without tensile capacity were retro-fitted to achieve adequate tensile capacity. In some cases additional micropiles were installed which had adequate tensile capacity to arrest foundation movements in the homes.

6. Conclusions

The authors offer the following conclusions regarding the use of grouted micropiles for underpinning of foundations on expansive soils.

- Grouted micropiles began to find substantial use in the United States as far back as the 1970's. Since that time they have been used for a wide variety of applications including use as a structural element to underpin foundations constructed on expansive soils.
- The design of grouted micropiles in expansive soils is complex due to the use of low friction casing, large length to diameter ratios and typically complex soil and wetting profiles. The use of finite element based solutions can be used to model pier heave and tensile force if the free-field heave and other input parameters are determined accurately.
- The depth and degree of wetting as they relate to the incremental free-field heave must be accurately determined for use in a formulation such as APEX to predict pier heave and tensile force in micropiles installed in expansive soil**.**
- Micropiles have distinct advantages as compared to alternative methods for underpinning of foundations on expansive soils. These advantages include ease of construction, ability to use the foundation as a reaction block on which to secure drilling equipment, ability to be installed in confined spaces and ability to be advanced to a specified design depth in stiff expansive soil.
- Care must be taken during construction to place the PVC casing specified by the design engineer and to securely attach the micropile to the foundation to limit both upward and downward vertical displacement.

7. References

Abdel-Halim, M.A.H. and Al-Qasem, M.M. (1995). "Model Studies on Bored Piles in Stiff Expansive Clay." *Int. J. of Structures*, 142(15), 35-59.

American Association of State Highway and Transportation Officials (AASHTO) (2012). "*Design Specifications Customary U.S. Units*." Publication Code LRFDUS-6.

Amir, J.M. and Sokolov, M. (1976). "Finite Element Analysis of Piles in Expansive Soils." *J. of Soil Mechanics and Foundation Engineering*, ASCE, 102(7), 701-719.

Benvenga, M. M. (2005). "Pier-Soil Adhesion Factor for Drilled Shaft Piers in Expansive Soil." Master's Thesis, Colorado State University, Fort Collins, Colorado (J.D. Nelson, advisor).

Chao, K. C., Overton, D. D., and Nelson, J. D. (2006). "The Effects of Site Conditions on the Predicted Time Rate of Heave." *Proc. of Unsaturated Soils Conf. 2006*. ASCE GSP147, 2086-2097.

Chen, F.H. (1965). "The Use of Piers to Prevent the Uplift of Lightly Loaded Structures Founded on Expansive Soils." *Proc. of the Int. Conf. on Expansive Soils*, College Station, Texas.

Chen, F. H. (1988). "*Foundations on Expansive Soils*." Elsevier. New York, NY.

Day, R.W. (1999). "Forensic Geotechnical and Foundation Engineering." The McGraw-Hill Companies. New York, NY.

Federal Highway Administration (FHWA) (2005*). "Micropile Design and Construction Reference Manual*." Publication No. NHI-05-039, NHI Course No. 132078, U.S. Dept. of Transportation. December.
Fredlund, D. G., Hasan, J. U., and Filson, H. (1980). "The Prediction of Total Heave." *Proc. 4th Int. Conf. on Expansive Soils,* Denver, Colorado, June 16-18, 1 – 11.
Fredlund, D. G. and Rahardjo, H. (1993). "*Soil Mechanics for Unsaturated Soils*." John Wiley & Sons, New York, NY.
Fredlund, D. G., Rahardjo, H. and Fredlund, M.D. (2012). "*Unsaturated Soil Mechanics in Engineering Practice*." John Wiley & Sons, Hoboken, NJ.
Houston, S. L., Houston, W., Zapata, C., and Lawrence, C. (2001). "Geotechnical Engineering Practice for Collapsible Soils." *Geotechnical and Geological Engineering*, 19(3-4), 333-355.
Justo, J.L., Saura, J., Rodriguez, J.E., Delgado, A. and Jaramillo, A. (1984). "A Finite Element Method to Design and Calculate Pier Foundations in Expansive-collapsing Soils." *Proc. of the 5th Int. Conf. on Expansive Soils*, Adelaide, Australia, 199-123.
Lambe, T.W and Whitman R.V. (1969). "*Soil Mechanics*." John Wiley & Sons, New York, NY.
Lytton, R.L. (1977). "Foundations in Expansive Soils." In *Numerical Methods in Geotechnical Engineering*, ed. C.S. Desai, and J.T. Christian, McGraw Hill Book Company, New York, NY. 427-457.
McWhorter, D. B. and Nelson, J. D. (1979). "Unsaturated Flow Beneath Tailings Impoundments." *J. Geotechnical and Engineering Division*, ASCE, November, 105(GT11), 1317-1334.
Mohamedzein, Y.E.A., Mohamed, M.G. and Sharief, A.M.E. (1999). "Finite Element Analysis of Short Piles in Expansive Soils." *Computers and Geotechnics*, 24, 231-243.
Nelson, J. D. and Miller, D. J. (1992). "*Expansive Soils: Problems and Practice in Foundation and Pavement Design*." John Wiley and Sons, New York, NY.
Nelson, J.D., Chao, K.C. and Overton, D.D. (2007). "Design of Pier Foundations on Expansive Soils." *Proc. of the 3rd Asian Conf. on Unsaturated Soils*, Nanjing, China.
Nelson, J. D., Chao, K. C., Overton, D. D. and Schaut, R. W. (2012a). "Calculation of Heave of Deep Pier Foundations." *SEAGS and AGSSEA Geotechnical Engineering J.*, 43(1).
Nelson, J. D., Overton, D. D., and Durkee, D. B. (2001). "Depth of Wetting and the Active Zone." *Proc.of the Geo-Institute Shallow Foundation and Soil Properties Committee Sessions at the ASCE Civil Eng. Conf. 2001*, Houston, Texas, October 10-13, in "Expansive Clay Soils and Vegetative Influence on Shallow Foundations" ed. C. Vipulanandan, M.B. Addison, and M. Hansen, GSP115, 95-109.
Nelson, J. D., Reichler, D. K., and Cumbers, J. M. (2006). "Parameters for Heave Prediction by Oedometer Tests." *Proc. of the 4th Int. Conf. on Unsaturated Soils.* Carefree, Arizona. April, GSP 147, 951 – 961.
Nelson, J. D., Thompson, E. G., Schaut, R. W., Chao, K. C., Overton, D. D., and Dunham-Friel, J. S. (2012b). "Design Considerations for Piers in Expansive Soils." *J. Geotechnical and Geoenvironmental Engineering*, ASCE, 138(8), 945-956.
Norrish, K. (1954). "The swelling of montmorillonite." *Discussions of the Faraday Society*, 18, 120–134.
O'Neill, M. W. (1988). "Special Topics in Foundations." *Proc. of the Geotechnical Engineering Division National Convention*, ASCE, Nashville, Tennessee, 1-22.
Overton, D. D., Chao, K. C., and Nelson, J. D. (2006). "Time Rate of Heave Prediction for Expansive Soils." *Proc. of GeoCongress 2006 Conf.* ASCE Atlanta, GA, February 26-March 1.

Poulos, H. G., and Davis, E. H. (1980). *Pile Foundation Analysis and Design*. John Wiley, New York, NY.
Reichler, D. K. (1997). *"Investigation of Variation in Swelling Pressure Values for an Expansive Soil."* Master's Thesis, Colorado State University, Fort Collins, Colorado.
Schaut, R.W., Nelson, J.D., Overton, D.D., Carraro, J.A.H. and Fox, Z.P. (2011). "Interface Testing for the Design of Micropiles in Expansive Soils." *Proc. of the 36th Annual Conf. on Deep Foundations*, Boston, MA, Oct 18-21, Deep Foundations Institute.
Sorochan, E.A. (1991). "*Construction of Buildings on Expansive Soils*." A.A. Balkema Publishers, Brookfield, VT.
U.S. Army Corps of Engineers. (1983). "Technical Manual TM 5-818-7, Foundations in Expansive Soils."